Polymer 51 (2010) 6248–6257

Contents lists available at ScienceDirect

Polymer

journal homepage: www.elsevier.com/locate/polymer

Temperature/pH-induced morphological regulations of shell cross-linked graft copolymer assemblies

Wen-Hsuan Chiang [a,b], Yuan-Hung Hsu [b], Fa-Fen Tang [b], Chorng-Shyan Chern [c], Hsin-Cheng Chiu [a,*]

[a] Department of Biomedical Engineering and Environmental Sciences, National Tsing Hua University, Hsinchu 300, Taiwan
[b] Department of Chemical Engineering, National Chung Hsing University, Taichung 402, Taiwan
[c] Department of Chemical Engineering, National Taiwan University of Science and Technology, Taipei 106, Taiwan

ARTICLE INFO

Article history:
Received 3 July 2010
Received in revised form
19 October 2010
Accepted 23 October 2010
Available online 30 October 2010

Keywords:
Self-assembly
Stimuli-responsive
Shell cross-linked

ABSTRACT

Shell cross-linked (SCL) assemblies are prepared from the thermally induced three-layered, onion-like micelles of graft copolymers comprising acrylic acid (AAc) and 2-methacryloylethyl acrylate (MEA) as the backbone units and poly(*N*-isopropylacrylamide) (PNIPAAm) and monomethoxy poly(ethylene glycol) (mPEG) as the grafts via radical polymerization of the MEA residues within the AAc-rich interfacial layers in the aqueous phase of pH 5.0 at 60 °C. The resulting nanosized SCL assemblies exhibit versatile structural regulations in a fully reversible manner in response to changes in pH and temperature. At 20 °C, SCL assemblies retain the morphology of vesicle-like hollow microspheres with pH-controlled water influx and particle size. At pH 7.0, SCL assemblies remain invariant in both vesicular structure and size irrespective of the temperature increase beyond the coil-to-globule phase transition of PNIPAAm grafts occurring primarily in a highly individual manner. When the temperature increases from 20 to 60 °C at pH 5.0, the hollow particle size is greatly reduced, accompanied by the development of hydrophobic, impermeable PNIPAAm lumens attached to the inside surfaces of the interfacial gel layers. In addition, SCL assemblies undergo a dramatic thermally induced transformation from the vesicle-like to micelle-like morphology by virtue of yielding hydrophobic PNIPAAm inner cores at pH 3.0. The thermally evolved morphology of SCL assemblies is governed by the vesicle structure in response to the effect of pH on the AAc ionization within the interfacial gel layers at ambient temperature.

1. Introduction

Stimuli-responsive colloidal assemblies attained from molecular packing of block or graft copolymers have shown attractive, unique characteristics in their supramolecular structures and stimuli-induced morphologic transformation [1–7]. By incorporating versatile functions into the well controlled assembly structures, development of such polymeric colloids mainly in the form of micelles or vesicles (polymersomes) exhibiting structural response to external stimuli is thus in great demand for innovative micro-carriers or microcontainers, which are useful in applications such as drug delivery and catalysis [8–15]. Taking advantage of recent advances in living radical polymerization techniques, various self-assembling colloids produced from block copolymers with tailored block lengths have been the primary focus of this pioneering research field [16–19].

Self-assembly of amphiphilic block copolymers occurring in aqueous media at concentrations above their critical aggregation concentrations, however, may disintegrate upon dilution in blood circulation after parenteral administration. Their prominent applications in drug delivery can thus be severely limited. Similarly, those stimulus (such as pH or temperature)-induced polymer assemblies may become unstable and undergo such structural variations as disintegration and dissolution upon dramatic changes in environmental conditions of the media [20–22]. To overcome this inherent problem, both shell cross-linking (SCL) [23–27] and core cross-linking (CCL) [28–31] of polymer micelles from block copolymers were proposed to enhance the structural stability during dilution. However, for stimulus-induced assemblies, the greatly improved structural stability is often achieved at the expense of the desired ability to structurally respond to external stimuli. For example, the reversible micelle/vesicle transition can be significantly impaired by micelle core cross-linking. While block copolymer chain segments in the core regions experience the transition from hydrophobic to hydrophilic state, development of transient hollow particle structure from SCL micelles evolved from the pH or temperature-induced

* Corresponding author. Tel.: +886 35750829; fax: +886 35718649.
E-mail address: hscchiu@mx.nthu.edu.tw (H.-C. Chiu).

0032-3861/$ – see front matter © 2010 Elsevier Ltd. All rights reserved.
doi:10.1016/j.polymer.2010.10.038

hydrophobic core structure in the aqueous phase was speculated [20]. There is no doubt that a reversible stimulus-responsive micelle/vesicle transition of functional assemblies as nanocarrier devices can effectively control the encapsulation and release of bioactive agents, either hydrophilic or hydrophobic. Nevertheless, very few studies demonstrated the self-assembly of copolymers capable of undergoing such dramatic structural rearrangement as reversible micelle/vesicle inversion in response to changes in either pH or temperature upon shell cross-linking [25].

It is thus our goal to develop functional SCL assemblies capable of evolving on demand various morphologies (including micelles and vesicles) in both structurally reversible and tunable manner. In this study, a facile and effective strategy employing dual pH/temperature responsive graft copolymers was proposed, primarily owing to the greatly enhanced compositional and structural feasibility in regulating assembly morphologies. Graft copolymers comprising acrylic acid (AAc) and 2-methacryloylethyl acrylate (MEA) units as the backbone and monomethoxy poly(ethylene glycol) (mPEG) and poly(*N*-isopropylacrylamide) (PNIPAAm) as the grafts were chosen for developing thermally induced micelles. While, at high temperature, the PNIPAAm chain segments act as the major component to control the thermally induced hydrophobic association, the mPEG grafts not only act as the coronae of colloidal particles to effectively prevent particles from aggregation but also spatially segregate the AAc-rich interfacial layers and hydrophobic PNIPAAm inner cores within the three-layered, onion-like micelle structure prior to shell cross-linking. The effects of mPEG grafts on prohibiting interactions of PNIPAAm chain segments with unionized AAc residues within the thermally induced micelles have been described in detail in our previous work [32]. The micelles were shell cross-linked via radical polymerization of the MEA moieties covalently attached to polymer backbones at high temperature and the response of the resultant SCL assemblies in structural transformation to external pH and temperature was studied in this work.

2. Experimental section

2.1. Synthesis of graft copolymers

Preparation of graft copolymers comprising AAc and MEA as the backbones and PNIPAAm and mPEG as the grafts was carried out as reported previously and described in detail in Supporting Information [2,32–34]. Two graft copolymers differing mainly in the MEA contents were employed. The MEA contents are 9.1 mol% (referred to as copolymer **A** hereinafter) and 19.1 mol% (**B**), respectively. Fig. 1a illustrates a representative ^{1}H NMR spectrum of copolymer **A** in $CDCl_3$ at ambient temperature along with the chemical structure and compositions. Detail structural characterization results of the copolymers are summarized in Table S1.

2.2. Preparation of SCL assemblies

The graft copolymer was dissolved to a concentration of 10.0 mg/mL in acetate buffer (pH 5.0, *I* 0.01 M) at 4 °C. The copolymer solution was subsequently passed through a 0.45 μm filter and purged with N_2 for 30 min. It was gradually heated to 60 °C and equilibrated at this temperature with stirring (100 rpm of the reciprocal shaking) for 12 h. The assemblies exhibiting a three-layered, onion-like micelle structure were then covalently stabilized by radical polymerization of the MEA residues under N_2 atmosphere for 72 h, using ammonium peroxydisulfate (APS) (0.6 mg/mL) as the initiator [32]. The aqueous solution of SCL assemblies was then subjected to ultrafiltration (Amicon 8200 with a Millipore PBMK membrane, MWCO 300000) against the acetate buffer at 4 °C to remove the copolymers that were not cross-linked.

2.3. Characterization

2.3.1. Dynamic and static light scattering (DLS and SLS) measurements

The z-average hydrodynamic particle diameters (D_h) and particle size distributions of the thermally induced polymeric micelles prior to SCL reaction and the subsequently SCL assemblies in aqueous solutions were determined mainly by a Malvern Zetasizer Nano-ZS instrument at 173° equipped with a 4 mW He–Ne laser operating at $\lambda = 632.8$ nm, using the cumulant analysis method [35]. The aqueous copolymer solution was passed through a 0.45 μm filter at 20 °C and equilibrated at 60 °C with stirring for 30 min prior to measurement. The mean particle sizes of SCL assemblies were determined in the temperature range 20–60 °C at varying pH adjusted by either 0.1 N NaOH or HCl. The sample was equilibriated at each preset temperature for 30 min. In degradation experiments, both the particle size and light scattering intensity of the SCL assemblies in aqueous solutions of pH 7.4 and *I* 0.15 M (37 °C) with incubation time were monitored by DLS. The data reported herein represent an average of at least triplicate measurements.

To assess the morphology of SCL assemblies as a function of temperature or pH in terms of the ratio of the gyration and hydrodynamic radii of the assemblies, the mean hydrodynamic radius (R_h) herein was attained by DLS on a Brookhaven BI-200SM goniometer equipped with a BI-9000 AT digital correlator using a solid-state laser (35 mW, $\lambda = 637$ nm) at 90°. The CONTIN algorithm method was employed for data analysis in order to confirm the absence of bimodal particle size distribution of the SCL assemblies with much enhanced reliability [35,36]. For determination of the root-mean-square radius of gyration (R_g) by SLS (BI-200SM goniometer), the excess absolute time-averaged scattered light intensity, known as the Rayleigh ratio R_θ, was approximated as

$$\left[\frac{KC}{R_\theta}\right] = \left[\frac{1}{M_W}\right]\left[1 + \frac{\left(R_g^2 q^2\right)}{3}\right] + 2A_2C \quad (1)$$

where the contrast factor, *K*, is given as $4\pi^2 n^2 (dn/dc)^2/(N_A\lambda_0^4)$ with N_A, *n*, λ_0, and dn/dc being Avogadro's number, the solvent refractive index, the wavelength of laser light, and the specific refractive index increment, respectively. A_2 is the second virial coefficient, *C* the polymer concentration (mg/mL) and *q* the magnitude of the scattering wave vector given by $q = (4\pi n/\lambda_0)\sin(\theta/2)$. By measuring R_θ for a set of *C* (0.025–0.1 mg/mL) and θ (30–150°), the apparent weight-average molar mass M_w and R_g of SCL assemblies under varying pH and temperature conditions can be estimated from Zimm plots [37]. Prior to the SLS measurements, the invariance of R_h of the SCL assemblies in the entire concentration range at the preset pH and temperature was confirmed by DLS. The dn/dc values of the aqueous solutions of SCL assemblies were obtained by a BI-DNDC differential refractometer ($\lambda = 620$ nm).

2.3.2. TEM structural examination

The sample was prepared by placing a few drops of aqueous solution of the SCL assemblies at 20 °C on a 300-mesh copper grid covered with carbon and allowed to stand for 20 s. Excess solution on the grid was gently removed with absorbent paper. This was followed by negative staining of the sample for 20 s using a uranyl acetate solution (5.0 wt%). The sample was then dried at 25 °C for 2 days. The TEM image was obtained on a JEOL JEM-1200 CXII microscope operating at an accelerating voltage of 120 kV.

2.3.3. Fluorescence measurements

Pyrene was used as a hydrophobic probe in fluorescence measurements. Aliquots (20.0 μL) of pyrene in acetone (3.0×10^{-5} M)

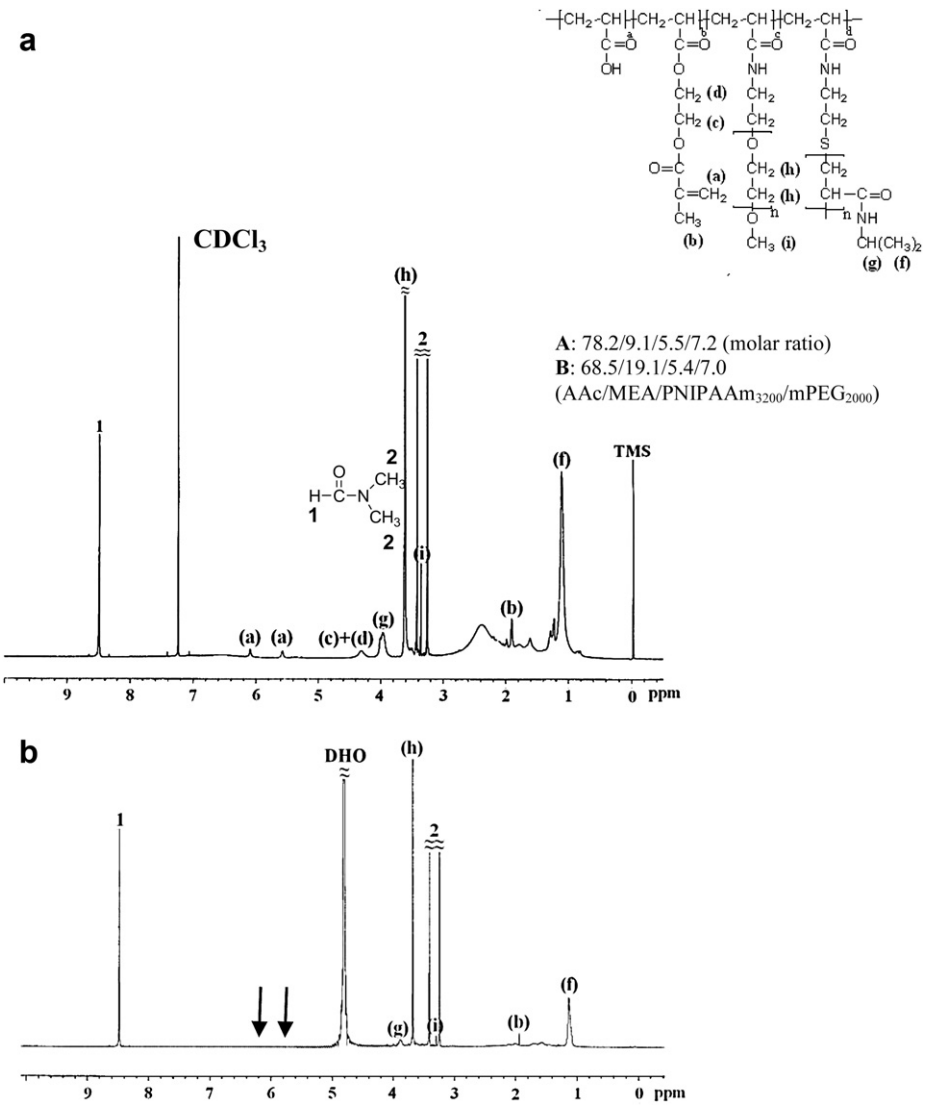

Fig. 1. ^{1}H NMR spectra of (a) graft copolymer **A** (10.0 mg/mL) in $CDCl_3$ and (b) SCL assemblies **A** (2.0 mg/mL) in D_2O at 20 °C. The assignment of the feature signals of the graft copolymers and the external standard (DMF) along with the chemical structure and compositions are also included.

were evaporated in vials, and the aqueous solutions of SCL assemblies at the prescribed pH (1.0 mL) were then added, yielding the SCL particle dispersions with a constant pyrene concentration of ca 6.0×10^{-7} M. The fluorescence intensity ratios (I_3/I_1) of the third vibronic band at 385.5 nm to the first at 373.5 nm of the fluorescence emission spectra of pyrene in the SCL particle dispersions at each preset temperature were determined [38]. The excitation was performed at 336 nm and the emission was recorded in the range from 350 to 500 nm on a Hitachi F-2500 fluorescence spectrometer equipped with a thermostat cell unit.

2.3.4. Variable temperature ^{1}H NMR characterization

A prescribed amount of lyophilized SCL assemblies (2.0 mg/mL) was suspended directly in D_2O (0.01 M NaCl). The pD of SCL particle dispersions was adjusted to the desired value by adding DCl or NaOD. ^{1}H NMR measurements of the SCL assemblies in D_2O from 20 to 60 °C were performed on a Varian Unity Inova-600 at 600 MHz without sample spinning. The pulse width of 4.9 s with a relaxation delay of 2 s was utilized. DMF in a sealed capillary was coaxially placed in the NMR sample tube as an external standard [2]. The proton signal of DMF at δ 8.45 ppm was employed as the resonance reference for assigning the feature signal positions and quantifying the signal integrals of SCL assemblies at different temperatures compared to the graft copolymer dissolved in $CDCl_3$ at ambient temperature. Prior to measurements, the sample was equilibrated at each preset temperature for 30 min.

3. Results and discussion

Detailed synthesis procedures used to prepare functional SCL assemblies from graft copolymers comprising AAc and MEA units as the backbone and PNIPAAm and mPEG as the grafts were described in the Supporting Information. It is, however, noteworthy that the absence of the Michael addition reaction presumably occurring between the primary amines of PNIPAAm-NH_2 and mPEG-NH_2 with the vinyl groups of MEA moieties has been confirmed by the essential constant MEA vinyl contents in copolymers before and after the grafting reactions [32]. In addition, the conjugation efficiencies greater than 90% (Fig. S2) indicate that the MEA content for the subsequent micelle shell cross-linking can be fully controlled. The grafting efficiencies for PNIPAAm and mPEG were ca 55% and 69%, respectively. Due to the presence of PNIPAAm

grafts, the copolymers that were dissolved completely at ambient temperature (10.0 mg/mL) underwent hydrophobic association and supramolecular assembly into micelles with the temperature being increased beyond the phase transition temperature of PINPAAm grafts (~34 °C) in the aqueous phase at pH 5.0. The D_h values of micelles **A** and **B** at 60 °C are ca 30 and 43 nm, respectively. The onion-like structure of the thermally induced micelles constituting distinct hydrophobic PNIPAAm inner cores, AAc-rich interfacial layers and mPEG coronae was clearly elucidated in our previous work [32].

SCL micelles were attained by radical polymerization of the MEA moieties residing within the AAc-rich interfacial layers at 60 °C and pH 5.0. APS was used as the initiator. The SCL reaction was successful, as evidenced by the complete disappearance of the ^{1}H NMR feature signals of the MEA vinyl protons at δ 5.7 and 6.5 ppm in D_2O at 20 °C and pD 5.0 (Fig. 1b and Fig. S7a), accompanied with the DLS single modal particle size distribution profiles of SCL assemblies **A** and **B** at 20 °C in aqueous solutions of both pH 5.0 and 7.0 (Fig. 2a). For comparison, the hydrodynamic particle sizes of copolymers **A** and **B** and the corresponding SCL assemblies at pH 5.0 and at 20 and 60 °C are summarized in Table S2. Being covalently stabilized, the assemblies fully retain their structural integrity without disintegration and dissolution below the lower critical solution temperature (LCST) of PNIPAAm grafts. The particle size of SCL assemblies **B** is slightly larger than that of **A**, irrespective of the external pH. This is primarily because the thermally induced micelles **B** are somewhat larger than **A** prior to the SCL reaction. Appreciable reductions in the ^{1}H NMR signal intensities of both the ethylene and methyl protons from the MEA moieties imply their reduced mobility within the SCL polymeric networks (interfacial gel layers). Note that DMF sealed in a capillary tube was repeatedly used as the external standard by placing it coaxially in the sample tube during NMR measurements. The proton signal from the formyl group of DMF at δ 8.45 ppm was selected as the reference resonance for evaluating the feature signal integrals in comparison with those obtained in $CDCl_3$ at ambient temperature. Fig. 2b shows the TEM images of SCL assemblies **A** at 20 °C and at pH 3.0, 5.0 and 7.0, respectively. By virtue of the effective radical polymerization of the MEA residues taking place exclusively within the AAc-rich interfacial layers, the SCL assemblies are well dispersed as individual spherical particles without any covalent interparticle connections at all three pH values. Similar to those reported previously [6,25,39], the TEM images seemingly display the SCL assemblies at 20 °C in hollow structure by the appearance of the clear contrast between the centers and the negatively stained shells with uranyl acetate. The assembly morphology was further characterized, particularly by SLS/DLS and variable temperature ^{1}H NMR measurements, as described below.

The response of SCL assemblies to changes in external pH at 20 °C in terms of the water influx is shown in Fig. 3. The water influx is defined as the increase of the mean hydrodynamic particle volume of SCL assemblies at each preset pH at 20 °C with respect to that of SCL assemblies at pH 3.0 and 60 °C, as shown below.

$$\text{Water influx} = \left(\frac{D_h}{D_{ho}}\right)^3 - 1 \quad (2)$$

where D_{ho} is the reference hydrodynamic diameter of SCL assemblies at pH 3.0 and 60 °C determined by DLS. At pH 3.0 and 60 °C, the SCL assemblies chosen as the reference for this study are assumed to have a nondraining micelle structure with negligible

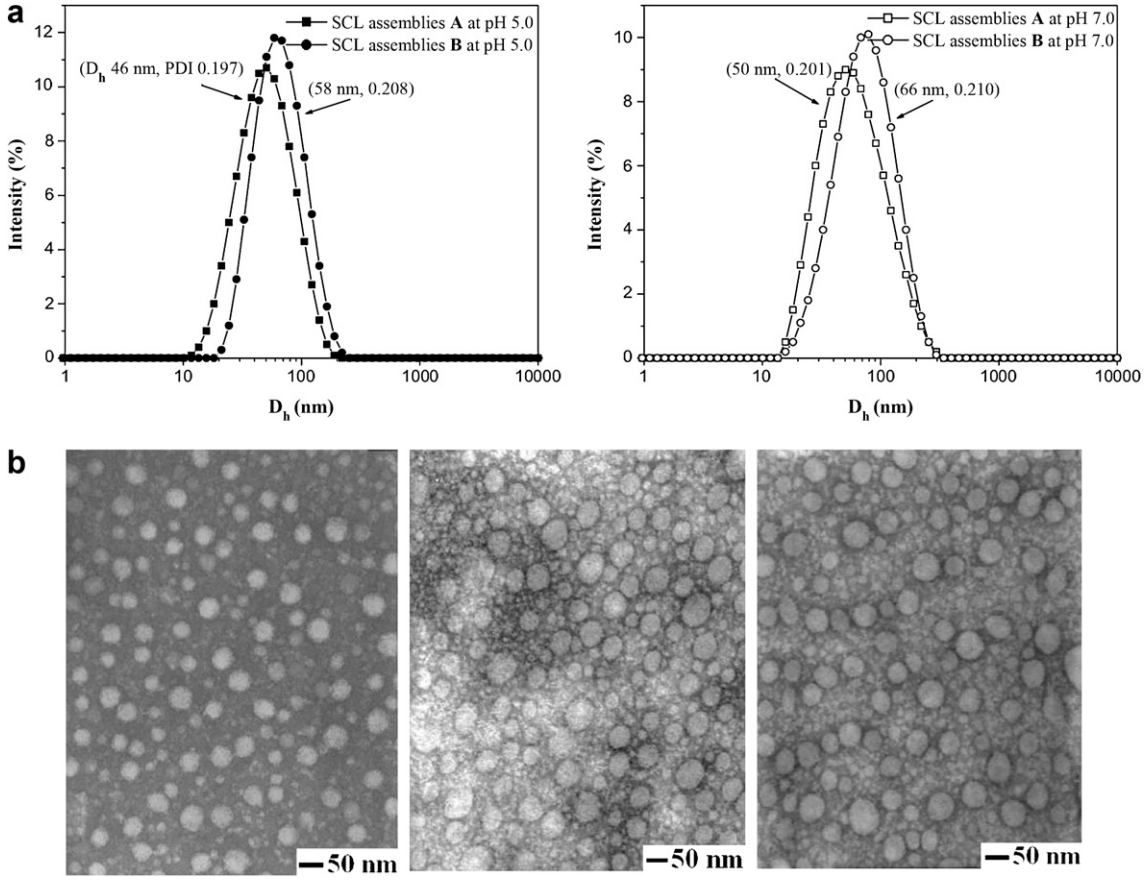

Fig. 2. (a) DLS colloidal size distribution profiles for SCL assemblies in aqueous solutions at 20 °C and (b) TEM images of SCL assemblies **A** at 20 °C and at pH 3.0, 5.0 and 7.0, respectively.

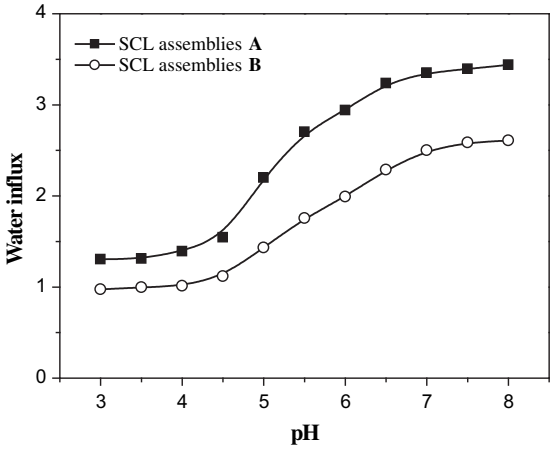

Fig. 3. pH dependence of water influx of SCL assemblies in aqueous solutions at 20 °C with respect to those at 60 °C and pH 3.0.

water influx (see the below description). The water influx into SCL assemblies **A** or **B** increases with increasing pH, particularly in the range from pH 4.0 to 7.0. This is primarily due to the increased ionization degree of the AAc residues within the cross-linked interfacial layers. This will enhance the interactions of the ionized AAc residues with water molecules and, thus, induce the development of ionic osmotic gradient via the accumulation of freely mobile ions within the cross-linked networks [40], thereby rendering the gel layers swollen and, in part, the particles enlarged. Due to the higher MEA content (19.1 mol%) and thus the higher SCL density of copolymer **B** than that of **A** (9.1 mol%), the SCL assemblies **B** show somewhat reduced water uptake at 20 °C in the pH range 3.0–8.0. However, only a small difference in water influx between assemblies **A** and **B** at pH 8.0 was observed. The variation in cross-linking densities derived presumably in a proportional manner from the initial MEA contents of copolymers **A** and **B** only shows a rather limited effect on the water uptake, which amounts to a total of at least 140% increase in the hydrodynamic particle volume of the assemblies when pH increases from 3.0 to 8.0. This is simply because the water influx is not only directed into the very thin interfacial layers where the cross-linking reaction occurred, but largely into the core regions in the absence of cross-linking at 20 °C, in which PNIPAAm grafts act as an osmotic attractor. This was partially verified by the estimation of the structural parameters of the SCL assemblies at the reference (dry) state based on the corresponding hydrodynamic particle size data (Fig. 4a), densities of PAAc (ρ_{PAAc}; 1.27 g/mL) and PNIPAAm ($\rho_{PNIPAAm}$; 1.08 g/mL) at pH 3.0 and 60 °C, and chemical compositions of copolymers **A** and **B** (Fig. 1a). Based on the assumptions of negligible water uptake by nondraining assemblies through the shell to core regions along with mPEG grafts being excluded from the main colloidal body and volume additivity, the mean radii of the hydrophobic cores and thicknessess of the interfacial gel layers can be calculated as follows:

$$R_{h,C} = R_{h,A} \times \left(\frac{M_{PNIPAAm}/\rho_{PNIPAAm}}{M_{PNIPAAm}/\rho_{PNIPAAm} + M_{PAAc/MEA}/\rho_{PAAc}} \right)^{1/3} \quad (3)$$

$$d_{SCL} = R_{h,A} - R_{h,C} \quad (4)$$

where $R_{h,C}$ is the hydrodynamic radius of the solid-like PNIPAAm core, $R_{h,A}$ the hydrodynamic radius of SCL assemblies and d_{SCL} the thickness of the cross-linked interfacial gel layer in aqueous solutions at pH 3.0 and 60 °C. The $M_{PNIPAAm}$ and $M_{PAAc/MEA}$ are the masses of the PNIPAAm grafts and PAAc-co-MEA backbones in graft copolymers (on the basis of 1.0 mol), respectively. The thickness of the PAAc shells is only ca 1.6 (or 2.6) nm compared to the inner core radius (13.5 (or 19.0) nm) of SCL assemblies **A** (or **B**). This implies that the hydration of core accounts significantly for the contribution of water influx to the particle enlargement, though this swelling process is initiated by the pH-induced AAc ionization within the interfacial layers. Accompanied with more ionized AAc units and concomitant disruption of hydrogen bonds among themselves within the gel layers and with PNIPAAm grafts on the inner layer surfaces, the cross-linked gel layers become more permeable for water influx into the inner core regions at higher pH. The increased tendency to reduce the curvature of nanoparticles with increasing charged AAc residues may further facilitate the enlargement of hydrodynamic particle volumes via water influx.

Fig. 4a shows the distinct responsive behaviors of SCL assemblies in the hydrodynamic particle diameter at pH 3.0, 5.0 and 7.0, respectively, to changes in temperature. Both SCL assemblies **A** and

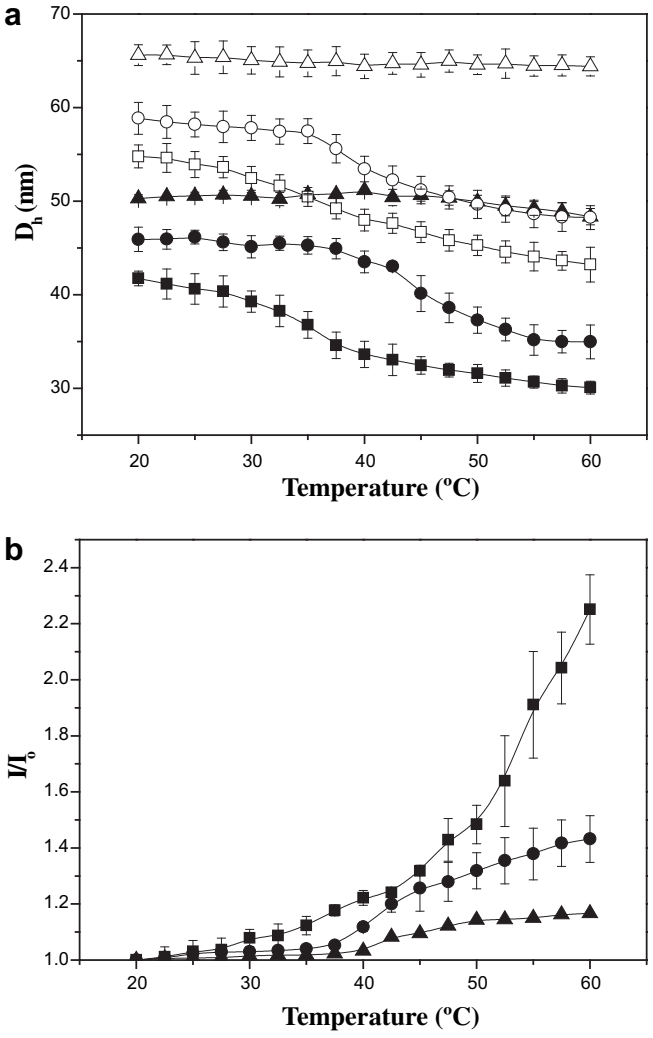

Fig. 4. (a) Mean hydrodynamic diameters (D_h) of SCL assemblies **A** (solid symbol) and **B** (open symbol) in aqueous solutions at pH 3.0 (■,□), 5.0 (●,○) and 7.0 (▲,△) as a function of temperature and (b) temperature dependence of light scattering intensity ratio (I/I_o) of SCL assemblies **A** in aqueous solutions at pH 3.0 (■), 5.0 (●) and 7.0 (▲). The I/I_o value of SCL assemblies was determined by DLS at each preset temperature to that at 20 °C. Error bars represent the standard deviation of triplicate measurements.

B show nearly identical temperature evolution profiles of the hydrodynamic particle size at three pH values. This indicates that a similar structural transition was achieved for these two assemblies in response to changes in temperature. At pH 7.0, D_h remains essentially unchanged irrespective of the temperature increase beyond the phase transition of PNIPAAm grafts, strongly implying the void of the required hydrophobic association in forming the PNIPAAm solid-like core regions. This is primarily due to the spatially enlarged internal aqueous compartments and, secondary, owing to the disruption of hydrogen bonds between the AAc units and PNIPAAm grafts at pH 7.0 that allows PNIPAAm grafts to reside within the compartments in a highly individual manner. Thus, the SCL assemblies retain their morphological structure as hollow microspheres at pH 7.0, independent of the external temperature change, though slight increases in the light scattering intensity ratio (I/I_o) determined by DLS at an onset temperature of 40 °C (Fig. 4b) suggest the coil-to-globule transition of individual PNIPAAm graft chain segments.

Nevertheless, SCL assemblies are capable of undergoing temperature-evolved structural transformation at pH 3.0 and 5.0 (Fig. 4a). The hydrodynamic particle size decreases appreciably with increasing temperature primarily as a result of the significant hydrophobic association and interchain aggregation of the PNIPAAm grafts residing within the enclosed internal aqueous chambers, thereby leading to water efflux and subsequent particle size reduction. At pH 3.0, the structural variation commences at an onset temperature (ca 25 °C) far below the LCST of PNIPAAm homopolymer in water, whereas a significant particle size reduction was observed at ca 35 °C with pH being increased from 3.0 to 5.0. This is mainly caused by the enhanced hydrophobic association of PNIPAAm chain segments arising from hydrogen bond pairings with unionized AAc residues on the inner shell surfaces at pH 3.0. It is noteworthy that the increased I/I_o with temperature at pH 3.0, particularly in the range from 45 to 60 °C, is different markedly from that at pH 5.0 (see Fig. 4b for SCL assemblies **A** and Fig. S4 for **B**). In general, the light scattering intensity of a colloidal system subjected to DLS measurements at a fixed angle relies intimately on the particle size, concentration, and structure. Owing to the fact that the hydrodynamic particle sizes are smaller and the concentrations are identical, the higher I/I_o values at pH 3.0 than those at pH 5.0 in the high temperature regime obviously reflect the formation of more nonpolar and compact solid-like structure. These data are in agreement with the results obtained from the fluorescence measurements of SCL assemblies in the aqueous phase using pyrene as a nonpolar probe. Fig. 5 shows the

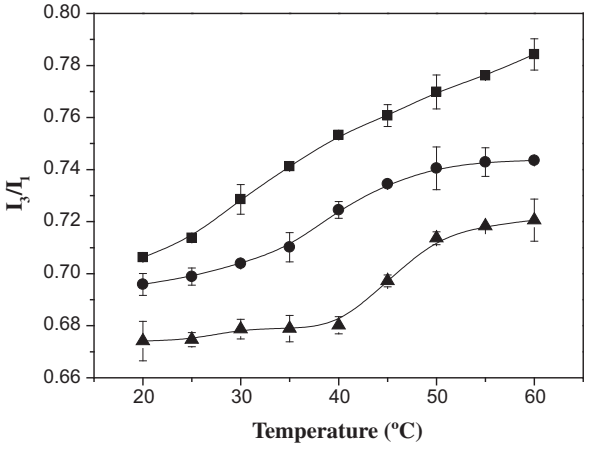

Fig. 5. Effect of temperature on the fluorescence intensity ratio I_3/I_1 of pyrene in aqueous solutions of SCL assemblies **A** at pH 3.0 (■), 5.0 (●) and 7.0 (▲). Error bars represent the standard deviation of triplicate measurements.

Table 1
DLS and SLS data for SCL assemblies A in aqueous phase.

pH	T (°C)	Rh (nm)[a]	Rg (nm)	Rg/Rh	Mw/10^6 (g/mol)
3.0	20	26.6	28.1	1.06	8.95
	45	23.5	19.2	0.82	9.23
	60	22.1	20.0	0.90	9.30
5.0	20	27.8	34.6	1.24	9.32
	45	25.0	30.0	1.20	8.90
	60	23.0	23.5	1.02	9.12
7.0	20	32.0	40.7	1.27	9.42
	45	32.8	42.0	1.28	9.15
	60	32.7	38.5	1.18	9.31

[a] Determined by DLS (Brookhaven BI-200SM) at a scattering angle of 90°, using the CONTIN analysis method.

temperature dependence of I_3/I_1 of SCL assemblies **A** at pH 3.0, 5.0 and 7.0, respectively (See Fig. S5 for **B**). The I_3/I_1 ratio represents a quantitative measure of the nonpolar nature of the microenvironments, in which pyrene resides [32,41]. The increased I_3/I_1 with temperature illustrates the enhanced hydrophobicity and phase transition of PNIPAAm grafts, while the onset temperature depends largely on their interactions with the pH-regulated unionized AAc residues. The varying fluorescence intensity ratio with pH, particularly at high temperatures, manifests the pronounced effect of the pH-controlled morphology of the cross-linked AAc-rich interfacial layers on the thermally induced hydrophobic association of PNIPAAm chain segments. The coil-to-globule phase transition of

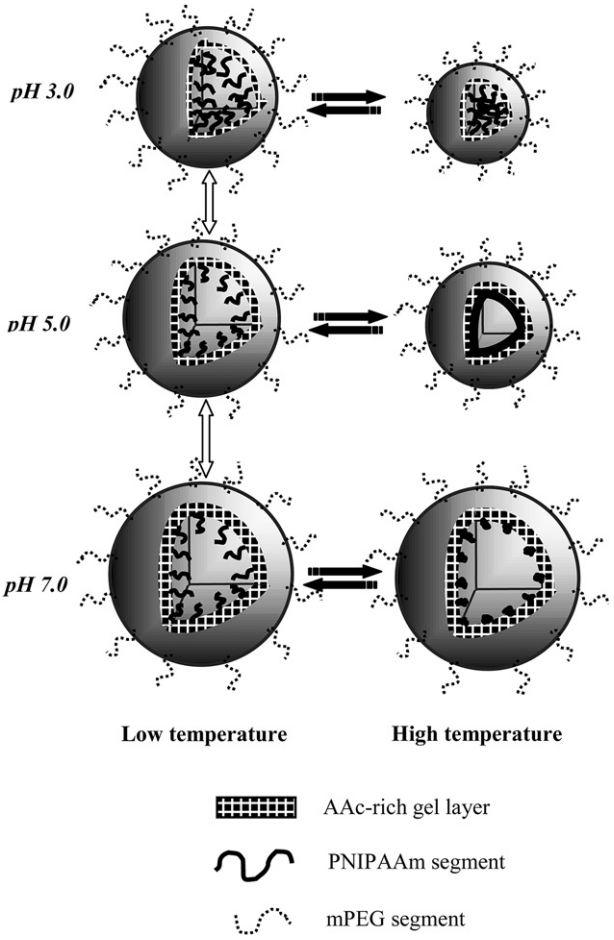

Scheme 1. Thermally evolved morphologic transformations of SCL assemblies at pH 3.0, 5.0 and 7.0.

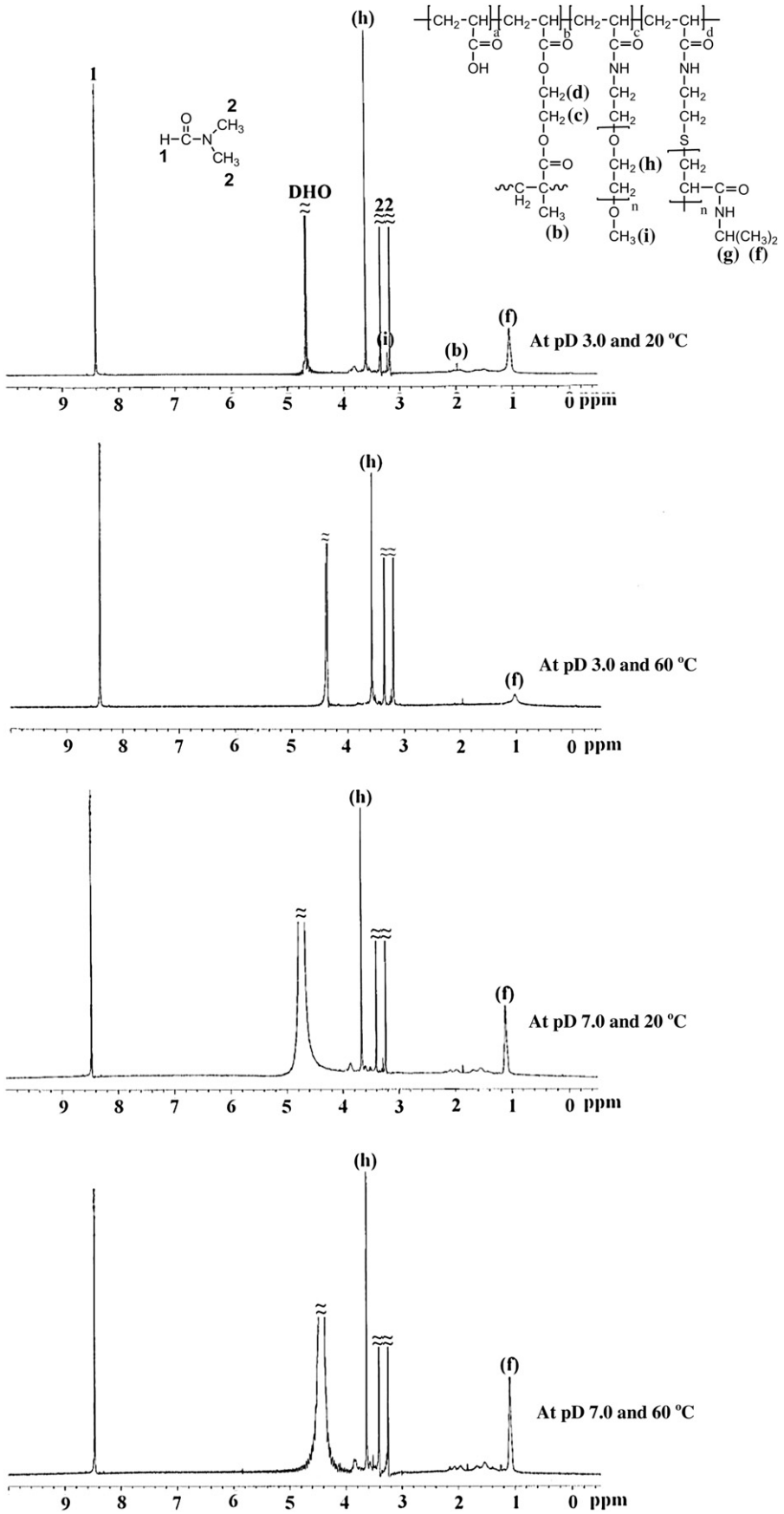

Fig. 6. ^{1}H NMR spectra of SCL assemblies **A** in D_2O (2.0 mg/mL) with varying pH and temperatures.

PNIPAAm grafts at pH 7.0 in a highly individual manner arising from the enlarged internal hollow microcages thus accounts for only a slight increase in I_3/I_1 when the temperature is raised to 60 °C.

In order to gain a fundamental insight into the structural variation of colloidal assemblies with changes in pH and temperature, SCL assemblies **A** were characterized by laser light scattering (LLS) at varying pH and temperatures and the results are summarized in Table 1. Note that the root-mean-square radius of gyration (R_g) obtained from the Zimm plot as illustrated in Fig S6 is strongly related to the mean distance of individual atoms (groups) that constitute the assembly of target to its mass center, while R_h is the radius of a hypothetical hard sphere that diffuses with the same speed as the target colloidal assembly under examination [36]. Based upon the particle form factors inherently associated with R_g and R_h, the R_g/R_h ratio is sensitive to assembly topology and thus useful for its structural justification [36,42–44]. With the pH being adjusted from 3.0 to 7.0 at ambient temperature, the R_g/R_h value varies from 1.06 to 1.27, thereby confirming the presence of assemblies in the form of vesicle-like hollow microspheres [43,44] and their capability of undergoing the transformation of the vesicle wall structure from dehydrated, compact and nondraining (at pH 3.0) to loose and swollen state (pH 7.0) [25]. At pH 7.0, the SCL assemblies are characterized by retaining the hollow microspherical structure with approximately identical particle size in the temperature range from 20 to 60 °C, though PNIPAAm grafts undergo the thermally induced coil-to-globule transition individually at high temperature.

At pH 5.0, the R_g/R_h values are reduced from 1.24 to 1.02 when the temperature increases from 20 to 60 °C, indicating the invariant morphology as vesicle-like hollow microspheres. However, the morphology is featured by developing a continuous and dense film that is closely attached to the inner surface of vesicle wall arising from the massive collapse of PNIPAAm grafts at high temperature, thereby rendering the vesicle wall impermeable and the particle size somewhat reduced. Interestingly enough, the SCL assemblies attained upon covalent cross-linking of the AAc-rich interfacial layer within the three-layered, onion-like micelles at 60 °C and pH 5.0 become incapable of re-establishing the micelle-like structure through the same heating process. Similar observation about the irreversible transformation of PNIPAAm chain segments from the micelle core to hydrophobic lumen of hollow spheres attained by the assembly of oppositely charged block copolymers was reported elsewhere [45]. This is attributed to a significant reduction in the chain flexibility and mobility of both PAAc backbones and tethered PNIPAAm grafts required in compliance with the formation of hydrophobic cores.

Being subjected to heating from 20 to 45 °C at pH 3.0, SCL assemblies were transformed from the vesicle-like to micelle-like structure by virtue of yielding nonpolar cores, thereby leading to a decrease in R_g/R_h to 0.82, a typical parameter for describing micelles [42,44,46]. As expected, upon the thermally induced transformation of SCL assemblies into the micelle-like structure, both the R_h and R_g values decrease accordingly. Furthermore, the dramatic decrease of R_g from 28.1 to 19.2 nm is a strong indication of the development of the hydrophobic solid-like inner cores. Apparently, the structural transformation of PNIPAAm grafts into either individual isolated globules, or continuous inner lumens, or nonpolar solid-like cores varies, depending largely upon the pH-controlled volume of the internal aqueous chambers of the hollow microspheres at 20 °C. With the colloidal particles being heated from 45 to 60 °C at pH 3.0, the R_g value slightly increases, while the R_h value decreases, thereby leading to an R_g/R_h value of 0.90. This is most likely caused by the stretch and subsequent dehydration of local mPEG chain segments spatially adjacent to the thermally induced outer surfaces of the colloidal particles [47,48]. Besides the geometric effect, the hydrogen bonding interactions of the partial mPEG chain segments with unionized AAc units and the hydrophobicity thus induced may also contribute to the dehydration process (see more related discussion below). The weight-average molecular weight of SCL assemblies is ca 9.2×10^6 g/mol, equivalent to ca 88 copolymer molecules within an assembly. In summary, the thermally evolved morphologic transformations of SCL assemblies at pH 3.0, 5.0 and 7.0 are illustrated in Scheme 1.

Fig. 6 shows the ^{1}H NMR spectra of SCL assemblies **A** in D_2O at pD 3.0 and 7.0. The thermally induced variation from 20 to 60 °C in the signal integrals of the methyl protons from PNIPAAm grafts at ca δ 1.1 ppm and the ethylene protons from mPEG grafts at 3.8 ppm changes with pH, as quantitatively illustrated in Fig. 7a and b. The thermally induced reduction of the feature methyl signal of PNIPAAm grafts signifies a quantitative measure of the chain segmental solidification due to a dramatic decrease in spin-lattice relaxation times (T_1) that renders the corresponding protons undetectable [2,33,34]. At pH 7.0, PNIPAAm grafts remain almost fully detectable regardless of the temperature increase beyond the phase transition region. This reflects the prominent hydration that allows each single PNIPAAm chain segment to experience the coil-to-globule transition (Fig. 7a) [49]. The ^{1}H NMR spectra of copolymer **A** and the corresponding SCL assemblies at pD 5.0 are shown in Fig. S7. In comparison with the ^{1}H NMR data for copolymer **A** without further cross-linking at pD 5.0 and particularly at high

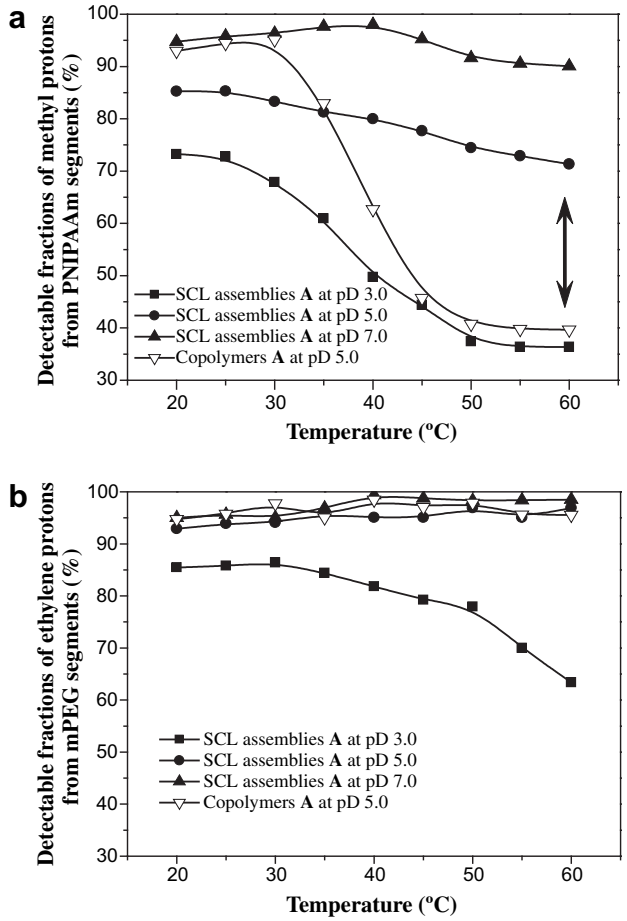

Fig. 7. Temperature evolved detectable fractions (%) of (a) the methyl protons from PNIPAAm and (b) the ethylene protons from mPEG chain segments of graft copolymers A (10.0 mg/mL) and the corresponding SCL assemblies (2.0 mg/mL) in D_2O in ^{1}H NMR measurements with respect to their signal integrals in $CDCl_3$ at 20 °C, using the DMF signal at δ 8.45 ppm as a reference.

temperatures (e.g., 60 °C), under which conditions these macromolecules were thermally evolved into micelles, the detectable PNIPAAm fractions of SCL assemblies are appreciably enhanced. This correlates well with the R_g/R_h values (Table 1), showing that, along with the thermal treatment at pH 5.0, PNIPAAm grafts of SCL assemblies are incapable of forming the hydrophobic core structure, but instead forming the continuous internal lumens. By contrast, the comparable detected fractions of PNIPAAm grafts of SCL assemblies at pH 3.0 and at temperatures higher than 45 °C with those of the thermally induced micelles in the absence of cross-linking at pH 5.0 were observed (Fig. 7a). This is in agreement with the depicted profiles of developing hydrophobic PNIPAAm inner cores within the SCL assembly structure by LLS characterization. In the low temperature region, PNIPAAm grafts were largely detected by ^{1}H NMR, which confirms the postulation of the extensive hydration of most PNIPAAm chain segments and the void of hydrophobic cores. At pH 3.0, the PNIPAAm detectable fraction was slightly reduced, which was in agreement with the LLS data of SCL assemblies in the nondraining vesicle-like structure (Table 1) and caused primarily by the enhanced hydrophobic effect of PNIPAAm chain segments complementary pairing with unionized AAc residues via hydrogen bonds. While serving as mobile coronae of the vesicle-like hollow assemblies, mPEG grafts remain fully detectable by ^{1}H NMR at pH 5.0 and 7.0 in the temperature range investigated in this work (Fig. 7b). The mPEG grafts of the SCL micelle-like assemblies, however, become partially undetected at 60 °C primarily as a consequence of the aforementioned local chain segmental stretch and solidification on the contracted particle surface area.

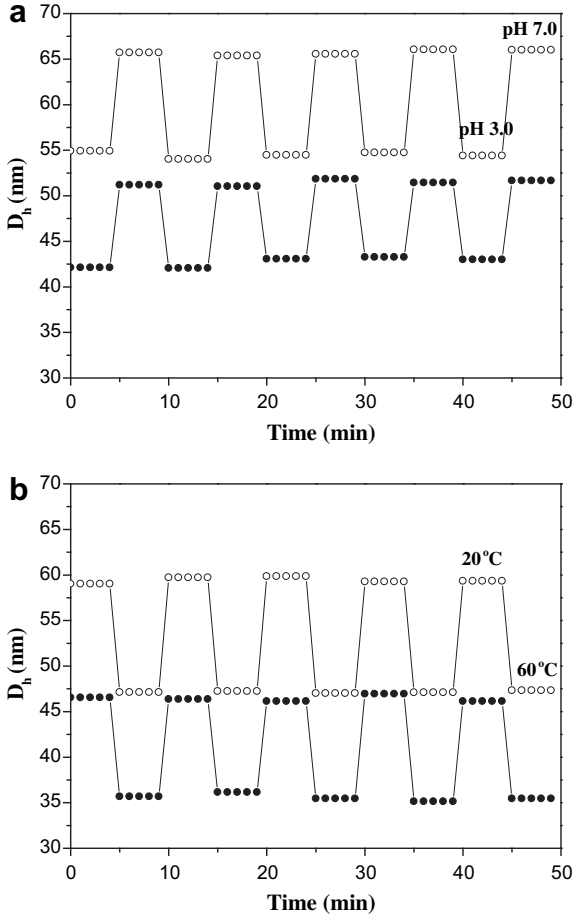

Fig. 8. Hydrodynamic particle size oscillation of SCL assemblies **A** (●) and **B** (○) between (a) pH 3.0 and 7.0 at 20 °C and between (b) 20 and 60 °C at pH 5.0 as determined by DLS.

It is noteworthy that the structural regulation of SCL assemblies in response to environmental stimuli behaves in a fully reversible manner. This can be seen by the prominent response of SCL assemblies to repeated abrupt changes in pH between 3.0 and 7.0 at 20 °C (Fig. 8a) and in the temperature range between 20 and 60 °C at pH 5.0 (Fig. 8b) with reversible oscillation of the hydrodynamic particle size in full magnitudes within 1 min. The rapid structural response of assemblies to external stimuli with either entire micelle/vesicle-like transformation or a full magnitude of almost 2-fold particle volume changes permits a precise and effective control of both the encapsulation and release of hydrophilic and/or hydrophobic cargoes. Based upon the chemical structure of SCL assemblies, the presence of two labile ester linkages in each of the MEA residues provides facile sites for the chemical disintegration of assemblies via hydrolysis. This greatly enhances the degradation feasibility of assemblies in such applications as pertinent stimuli-responsive nanocarrier devices for drug delivery. The representative degradation profiles of SCL assemblies **A** in aqueous buffer of pH 7.4 at 37 °C in terms of changes in hydrodynamic particle size with time are shown in Fig. S8.

Taking advantage of the enhanced compositional and structural feasibility of graft copolymers, this work demonstrates that, through the pertinent design of the molecular architecture, copolymer assemblies attained by shell cross-linking of the thermally evolved three-layered, onion-like micelles can promote not only the assembly integrity but also the structural susceptibility to external stimuli. With the unique stimuli-induced morphologic regulations, including both the dramatic micelle/vesicle inversion and fine modulation of vesicle wall structures, such a nanosized assembly system shows great potential as artificially intelligent biofunctional encapsulants to provide facile controls in both the encapsulation and release of bioactive target cargoes (either hydrophilic or hydrophobic) simply by the manipulation of external pH and temperature.

4. Conclusion

Two SCL assembly systems with different cross-linking densities originating from graft copolymers comprising AAc and MEA as the backbone and PNIPAAm and mPEG as the grafts were synthesized and characterized. Owing to the inherent LCST property of PNIPAAm grafts, these copolymers underwent the thermally induced hydrophobic association into three-layered, onion-like micelles that were subsequently subjected to covalent structure stabilization via radical polymerization of the MEA residues within the AAc-rich interfacial layers in the aqueous phase of pH 5.0 at 60 °C. The resultant SCL assemblies showed the capability of undergoing versatile structural transformation in a fully reversible manner in response to changes in pH and temperature. At 20 °C, SCL assemblies retain the morphology of vesicle-like, hollow microspheres with varying water influxes and thus particle sizes virtually governed by the external pH. While the hollow microspheres at pH 3.0 are nondraining, SCL assemblies commence water uptake as the extent of the pH-controlled AAc ionization within the interfacial gel layers increases, particularly in the pH range from 4.0 to 7.0. At pH 7.0, SCL assemblies remain unchanged in terms of both the vesicular structure and size irrespective of the temperature increase beyond the coil-to-globule phase transition of PNIPAAm grafts occurring primarily in a highly individual manner. With the temperature being increased from 20 to 60 °C, the vesicle-like structure at pH 5.0 remains the same but with an appreciable reduction in the particle size (by water efflux) and the development

of hydrophobic, impermeable PNIPAAm lumens attached to the inside surfaces of the AAc-rich interfacial gel layers. While subjected to the thermal treatment at pH 3.0, SCL assemblies undergo a dramatic transformation from the vesicle-like to micelle-like morphology by virtue of yielding hydrophobic PNIPAAm inner cores at an onset temperature far below the LCST of PNIPAAm alone primarily as a result of the enhanced hydrophobic association induced by the complementary hydrogen bonding pairings of PNIPAAm chain segments with unionized AAc residues on the inner surfaces of the interfacial gel layers. The thermally evolved morphology of SCL assemblies is essentially governed by the vesicle structure in response to the effect of external pH on the AAc ionization within the interfacial gel layers at ambient temperature.

Acknowledgment

This work is supported by the National Science Council of Taiwan.

Appendix. Supporting information

Supplementary data related to this article can be found online at doi:10.1016/j.polymer.2010.10.038

References

[1] Zhang BY, He WD, Li WT, Li LY, Zhang KR, Zhang H. Polymer 2010;51(14):3039–46.
[2] Hsu YH, Chiang WH, Chen CH, Chern CS, Chiu HC. Macromolecules 2005;38(23):9757–65.
[3] Li G, Shi L, Ma R, An Y, Huang N. Angew Chem Int Ed 2006;45(30):4959–62.
[4] Guragain S, Bastakoti BP, Yusa S, Nakashima K. Polymer 2010;51(14):3181–6.
[5] Cheng L, Zhang G, Zhu L, Chen D, Jiang M. Angew Chem Int Ed 2008;47(52):10171–4.
[6] Sundararaman A, Stephan T, Grubbs RB. J Am Chem Soc 2008;130(37):12264–5.
[7] Chiu HC, Lin YW, Huang YF, Chuang CK, Chern CS. Angew Chem Int Ed 2008;47(10):1875–8.
[8] Napoli A, Valentini M, Tirelli N, Muller M, Hubbell JA. Nat Mater 2004;3(3):183–9.
[9] Wang H, An Y, Huang N, Ma R, Li J, Shi L. Macromol Rapid Commun 2008;29(16):1410–4.
[10] Iatrou H, Frielinghaus H, Hanski S, Ferderigos N, Ruokolainen J, Ikkala O, et al. Biomacromolecules 2007;8(7):2173–81.
[11] Zhang L, Guo R, Yang M, Jiang X, Liu B. Adv Mater 2007;19(19):2988–92.
[12] Lee Y, Ishii T, Cabral H, Kim HJ, Seo JH, Nishiyama N, et al. Angew Chem Int Ed 2009;48(29):5309–12.
[13] Broz P, Driamor S, Ziegler J, Ben-Haim N, Marsch S, Meier W, et al. Nano Letters 2006;6(10):2349–53.
[14] Onaca O, Enea R, Hughes DW, Meier W. Macromol Biosci 2009;9(2):129–39.
[15] Lu J, Li N, Xu Q, Ge J, Lu J, Xi X. Polymer 2010;51(8):1709–15.
[16] Won YY, Davis HT, Bates FS. Science 1999;283(5404):960–3.
[17] Discher DE, Ahmed F. Annu Rev Biomed Eng 2006;8(1):323–41.
[18] Smith AE, Xu X, Abell TU, Kirkland SE, Hensarling RM, McCormick CL. Macromolecules 2009;42(8):2958–64.
[19] Yusa SI, Yokoyama Y, Morishima Y. Macromolecules 2009;42(1):376–83.
[20] Read ES, Armes SP. Chem Commun 2007;29:3021–35.
[21] Jiang X, Ge Z, Xu J, Liu H, Liu S. Biomacromolecules 2007;8(10):3184–92.
[22] Chang C, Wei H, Feng J, Wang ZC, Wu XJ, Wu DQ, et al. Macromolecules 2009;42(13):4838–44.
[23] Thurmond KB, Kowalewski T, Wooley KL. J Am Chem Soc 1996;118(30):7239–40.
[24] Li Y, Du J, Armes SP. Macromol Rapid Commun 2009;30(6):464–8.
[25] Dou H, Jiang M, Peng H, Chen D, Hong Y. Angew Chem Int Ed 2003;42(13):1516–9.
[26] Weaver JVM, Tang YQ, Liu SY, Iddon PD, Grigg R, Billingham NC, et al. Angew Chem Int Ed 2004;43(11):1389–92.
[27] Jin Q, Liu X, Liu G, Ji J. Polymer 2010;51(6):1311–9.
[28] Liu X, Jiang M. Angew Chem Int Ed 2006;45(23):3846–50.
[29] Zhang J, Zhou Y, Zhu Z, Ge Z, Liu S. Macromolecules 2008;41(4):1444–54.
[30] Zhang Y, Gu W, Xu H, Liu S. J Polym Sci A Polym Chem 2008;46(7):2379–89.
[31] Zheng G, Zheng Q, Pan C. Macromol Chem Phys 2006;207(2):216–23.
[32] Chiang WH, Hsu YH, Lou TW, Chern CS, Chiu HC. Macromolecules 2009;42(10):3611–9.
[33] Hsu YH, Chiang WH, Chen MC, Chern CS, Chiu HC. Langmuir 2006;22(16):6764–70.
[34] Chiang WH, Hsu YH, Chern CS, Chiu HC. J Phys Chem B 2009;113(13):4187–96.
[35] Chen K, Ballas SK, Hantgan RR, Kim-Shapiro DB. Biophys J 2004;87(6):4113–21.
[36] Schartl W, editor. Light scattering from polymer solutions and nanoparticle dispersions. Heidelberg, Germany: Springer-Verlag; 2007 [Chapter 4].
[37] Luo S, Xu J, Zhang Y, Liu S, Wu C. J Phys Chem B 2005;109(47):22159–66.
[38] Kalyanasundaram K, Thomas JK. J Am Chem Soc 1977;99:2039–44.
[39] Qian J, Wu F. Macromolecules 2008;41(22):8921–6.
[40] Chiu HC, Lin YF, Hung SH. Macromolecules 2002;35(13):5235–42.
[41] Yang Z, Zhang W, Zou J, Shi W. Polymer 2007;48(4):931–8.
[42] Niu AZ, Liaw DJ, Sang HC, Wu C. Macromolecules 2000;33(9):3492–4.
[43] Zhang W, Zhou X, Li H, Fang Y, Zhang G. Macromolecules 2005;38(3):909–14.
[44] Wei H, Wu DQ, Li Q, Chang C, Zhou JP, Zhang XZ, et al. J Phys Chem C 2008;112(39):15329–34.
[45] Li Z, Xiong D, Xu B, Wu C, An Y, Ma R, et al. Polymer 2009;50(3):825–31.
[46] Liu S, Weaver JVM, Tang Y, Billingham NC, Armes SP, Tribe K. Macromolecules 2002;35(16):6121–31.
[47] Hu T, Wu C. Macromolecules 2001;34(19):6802–5.
[48] Chen H, Zhang Q, Li J, Ding Y, Zhang G, Wu C. Macromolecules 2005;38(19):8045–50.
[49] Wu C, Zhou S. Macromolecules 1995;28(24):8381–7.